RAA 2020 Vol. **20** No. **3**, 43(7pp) doi: 10.1088/1674–4527/20/3/43

http://www.raa-journal.org *http://iopscience.iop.org/raa*

Research in Astronomy and Astrophysics

Binary star detection in the open cluster King 1 field

Parvej Reja Saleh[1], Debasish Hazarika[1], Ajaz Ahmad Dar[2], Padmakar Singh Parihar[3] and Eeshankur Saikia[1]

[1] Department of Applied Sciences, Gauhati University-781014, Assam, India; *prvzslh@gauhati.ac.in*
[2] Department of Physics, University of Kashmir-190006, Srinagar-J&K, India
[3] Indian Institute of Astrophysics, Koramagala-560034, Bangalore, India

Received 2019 September 8; accepted 2019 November 21

Abstract A rarely studied open cluster, King 1 is observed using the 1.3-m telescope equipped with a $2\mathrm{k}\times4\mathrm{k}$ CCD at Vainu Bappu Observatory, India. We analyze the photometric data obtained from CCD observations in both B and V bands. Out of 132 detected stars in the open cluster King 1 field, we have identified four stellar variables, and two among them are reported as newly detected binary systems. The parallax values from Gaia DR2 suggest that the open cluster King 1 is in the background of these two detected binary systems, falling along the same line of sight, giving rise to different parallax values. Periodogram analysis was carried out using Phase Dispersion Minimization (PDM) and the Lomb-Scargle (LS) method for all the detected variables. PHysics Of Eclipsing BinariEs (PHOEBE) is extensively employed to model various stellar parameters of both the detected binary systems. Based on the modeling results obtained from this work, one of the binary systems is reported for the first time as an Eclipsing Detached (ED) and the other as an Eclipsing Contact (EC) binary of W-type W UMa.

Key words: galaxies: photometry — galaxies: clusters: individual (King 1) — (stars:) binaries: eclipsing — methods: observational

1 INTRODUCTION

To study stellar evolution, open clusters are among the best objects, as they provide vital information about their distance, age, composition and masses. Numerous types of variable stars are present in a star cluster because of their transition through various stages of evolution (Lata et al. 2011). A very rarely observed open cluster, King 1, discovered by King (1949) in the second Galactic quadrant near the Perseus spiral arm, was initially investigated through photometric study in $UBVRI$ bands by Lata et al. (2004). Their study reports a broad main sequence in the color-magnitude diagram and a Galactic radius of $4'$, derived from their density of stellar surface. They also estimated the age, distance modulus and reddening to be 1.6 ± 0.4 Gyr, $(m-M)_0 = 11.38$ mag and $E(B-V) = 0.70 \pm 0.05$ mag respectively, based on the isochrone fitting, considering solar metallicity. Soon after, Maciejewski & Niedzielski (2007) reported the same parameters to be ~ 4 Gyr, $(m-M)_0 = 10.17^{+0.32}_{-0.51}$ mag and $E(B-V) = 0.76 \pm 0.09$ mag respectively. Also, from the VI photometry of King 1, Hasegawa et al. (2008) reported the age, distance modulus and reddening to be 2.8 Gyr, $(m-M)_0 = 11.57$ mag and $E(B-V) = 0.62$ mag respectively. In Carrera et al. (2017), the same parameters were estimated with both photometric and spectroscopic observations and were reported as 2.8 ± 0.3 Gyr, $(m-M)_0 = 10.6 \pm 0.1$ mag and $E(B-V) = 0.80 \pm 0.05$ mag respectively. Additionally, they estimated the central location of the open cluster King 1 at $\mathrm{RA} = 00^{\mathrm{h}}22^{\mathrm{m}}$ and $\mathrm{Dec} = +64^\circ 23'$ with an uncertainty of $\sim 1'$. A central density and a core radius were also computed to be 6.5 ± 0.2 star arcmin^{-2} and $1.'9 \pm 0.'2$ respectively. Later, Lata et al. (2014) updated the age, distance, reddening and linear diameter to be $\log(\mathrm{Age}) = 9.2 \pm 0.1$, 1.9 kpc, $E(B-V) = 0.70 \pm 0.05$ mag and 4.3 pc respectively using $UBVRI$ charge-coupled device (CCD) photometry. However, an inconsistency in the age, distance modulus and reddening can be clearly seen in the reported results so far.

Since the open cluster King 1 has been less studied and no previous reports were found so far with the specific goal of detecting stellar variables, our main motivation in this work was to explore the stellar variability and investigate the presence of binary stars within the field of view (FoV) of the open cluster King 1. These findings definitely add value to the existing studies of this open cluster, and al-

Table 1 Observation Log of the Open Cluster King 1

Observation Nights	Bands	No. of Frames	Exposure (s)
05–11–2017	B, V	26	600, 600
06–11–2017	B, V	09	600, 600
07–11–2017	B, V	21	600, 600
08–11–2017	B, V	17	600, 600
09–11–2017	B, V	22	600, 600
10–11–2017	B, V	27	600, 600
11–11–2017	B, V	21	600, 600

so similar others. The physical characteristics of the stars, such as mass, light, temperature and abundance, play a significant role in studying the pulsating stars, as this type of star occurs with a wide range of parameters and evolutionary phases.

This paper is organized as follows - the observational analysis and data reduction are described in Section 2. The process of detecting the variable stars and their respective light curves is presented in Section 3. In Section 4, multiple period detection methods are performed on the variable stars. In Section 5, the results are summarized, which discuss the phase plots, color-magnitude diagrams and photometric solutions obtained from the PHysics Of Eclipsing BinariEs (PHOEBE) modeling of the detected binary stars.

2 PHOTOMETRIC OBSERVATIONS AND DATA ANALYSIS

Photometric observations of the open cluster King 1 were carried out for both the B and V bands at Vainu Bappu Observatory, Kavalur from 2017 November 5 to 11, using a 1.3-m telescope. The $2\mathrm{k} \times 4\mathrm{k}$ CCD with FoV of ~ 0.3 arcsec pixel^{-1}, readout noise of ~ 4.2 electrons and gain $0.745\,\mathrm{e}^{-1}\mathrm{ADU}^{-1}$ was utilized to monitor the cluster. We have recorded bias, flat and object frames for each night. The images in B and V filters were taken with long exposure times. Table 1 provides the details of the observation log.

The CCD frames were cleaned and pre-processed in Image Reduction and Analysis Facility (IRAF) to recognize available bright stars in our field. By considering the image shift and rotation, we computed the coordinates of the detected stars with respect to a reference frame. The reference frame was selected after a visual inspection of all the 143 object frames, which have overall the best photographic qualities among the ones we examined. DAOPHOT (Stetson 1987) was applied to detect the stars and generate its respective coordinates for every frame. The coordinates are used in DAOPHOT-II's PHOT task as an input to aperture photometry. The data files with night frames including all the scientific data, such as flux and magnitude with errors of all marked stars, are dumped into the DAOPHOT (PHOT) output. A maximum number of star fluxes was taken into consideration for computing standard deviation. The stars with lesser standard deviations were considered as comparison stars. Python programming was extensively employed to develop this algorithm. Stars with larger standard deviations were discarded. This process is iterative and is continued until the remaining stars are found to be non-variable, i.e., smaller standard deviations (Dar et al. 2018a,b). Following Kiss et al. (2001); Kang et al. (2007); Wang et al. (2015), the instrumental magnitudes of each detected star in all the frames were utilized to compute the standard magnitudes respectively. Among 132 detected stars, we have selected four unsaturated bright stars, having smaller standard deviations for differential photometry, as displayed in Figure 1. These stars are not located in any of the edges of the CCD frames. Gilliland & Brown (1988)'s ensemble normalization was applied to normalize instrumental magnitudes of the V band.

3 VARIABLE STAR DETECTION

The presence of variability in 132 detected stars was visually inspected from all light curves. We searched for characteristics, such as eclipses of binaries, planetary transits and pulsations with elevated amplitude. Figure 2 reflects the standard deviation in V band depending on the instrumental magnitude. Out of 132 stars in the King 1 field, four variables were detected with higher standard deviations as compared to the other non-variable stars. These four objects have also been observed by Two Micron All-Sky Survey (2MASS)[1] and Gaia Data Release 2 (DR2[2]). 2MASS reported their precise positions (RA, Dec) and brightness information in the infrared bands, i.e., J (1.25 microns), H (1.65 microns) and Ks (2.17 microns), whereas Gaia DR2 provided the parallaxes, proper motions, radial velocity information and G-band magnitudes (Gaia Collaboration et al. 2018). The 2MASS and Gaia DR2 IDs of the reported four variables are mentioned in Table 2.

The FoV of the open cluster King 1 was calibrated with the available catalogs, viz. 2MASS and Gaia DR2, where the header of one of the CCD frames was updated with the World Coordinate System (WCS). WCS in the header allows us to extract the RA and Dec of each star present in a CCD frame. To compute the WCS, a plate solution was created implementing the IRAF packages *ccmap* and *ccsetwcs*. SAOImage DS9 was extensively applied to perform this process, where the Gaia DR2 catalog (Gaia Collaboration et al. 2018) was referenced to match the position of our CCD frame.

[1] *https://irsa.ipac.caltech.edu/Missions/2mass.html*

[2] *https://www.cosmos.esa.int/web/gaia*

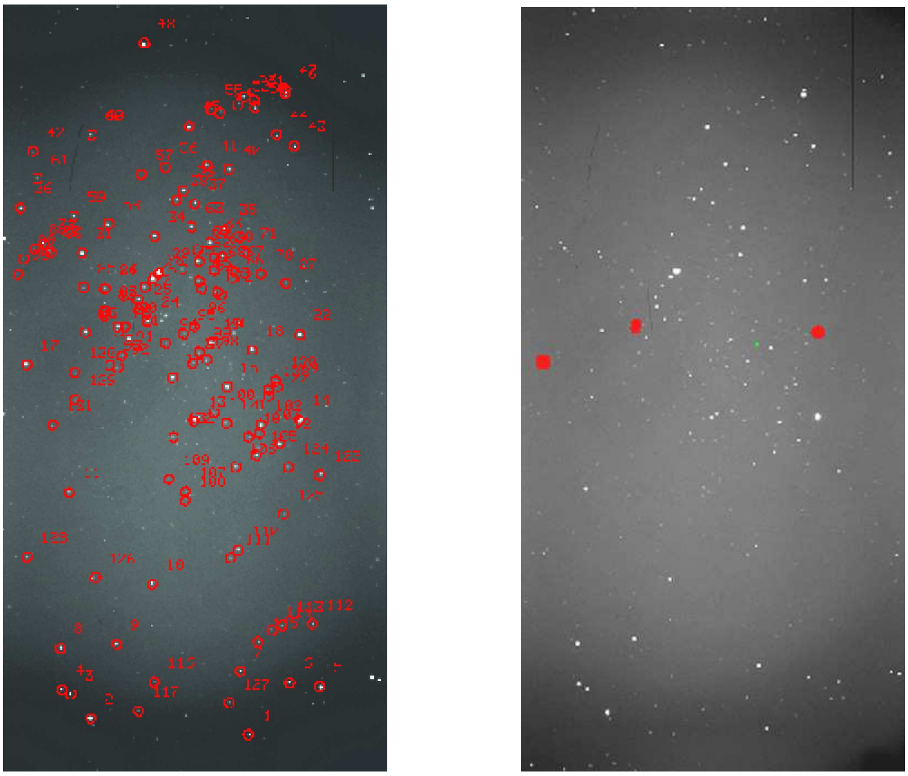

(a) 132 stars (b) 4 variables

Fig. 1 (a) Photometric frames of King 1 field, marked with the detected stars; (b) Among the detected stars, variable stars are marked.

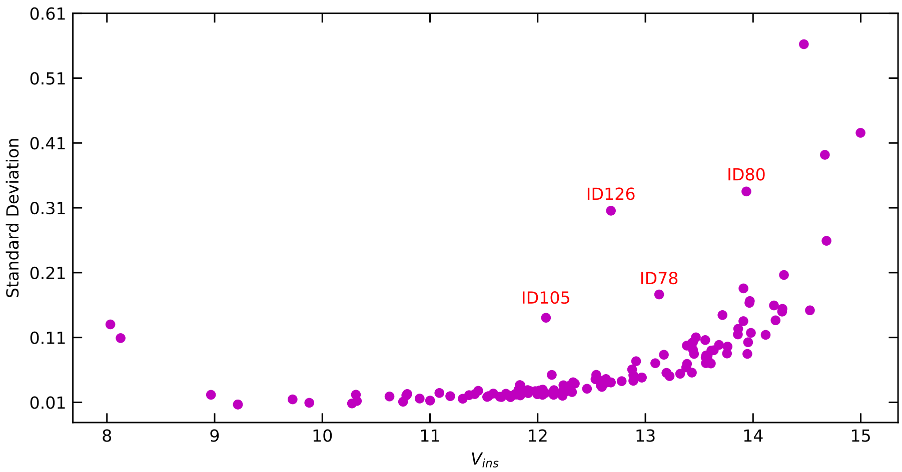

Fig. 2 Standard deviation vs. magnitude-averaged mean V magnitude of 132 detected stars in the King 1 field. The *marked stars* are variables with relatively higher standard deviations, ignoring the outliers, which are considered for further analysis.

The parallax of the 132 stars present in the CCD frame is taken into account. It demonstrates that there are few objects which do not belong to King 1. Lata et al. (2014) estimated the distance to King 1 as 1.9 kpc, which corresponds to a parallax of ~ 0.5263 mas. Notably, ID78 and ID80 have parallaxes of 0.5430±0.0285 mas and 0.5529±0.0755 mas respectively, supporting their existence within the open cluster. However, the two reported binaries ID105 and ID126, with parallaxes of 2.3568±0.0706 mas and 3.6268±0.0621 mas respectively, seem to be far in front of King 1, though along its line of sight. Nevertheless, we have extended our work on these two binary stars, as no previous discussions on their characteristics are reported.

4 PERIOD DETERMINATION

To obtain the most probable periods, we have employed two methods, viz. Phase Dispersion Minimization (PDM)

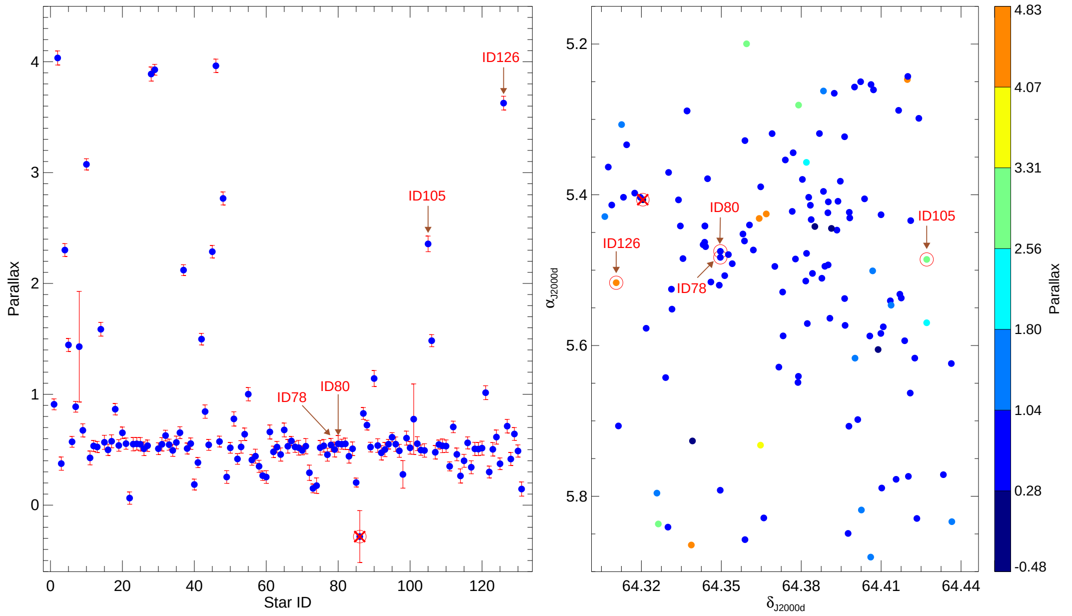

(a) Parallax from GAIA DR2 (b) RA Dec vs Parallax

Fig. 3 (a) The parallax, in milliarcseconds (mas), of the 132 detected stars in the CCD frame considered along with its error is depicted here. Most of the objects lie in the parallax range from 0 to 1, which includes ID78 and ID80. However, there are few objects possessing higher parallax, including ID105 and ID126. The object marked as ⊗ has a negative parallax as reported by Gaia DR2. (b) The RA and Dec mapping of the 132 detected stars with their parallax values.

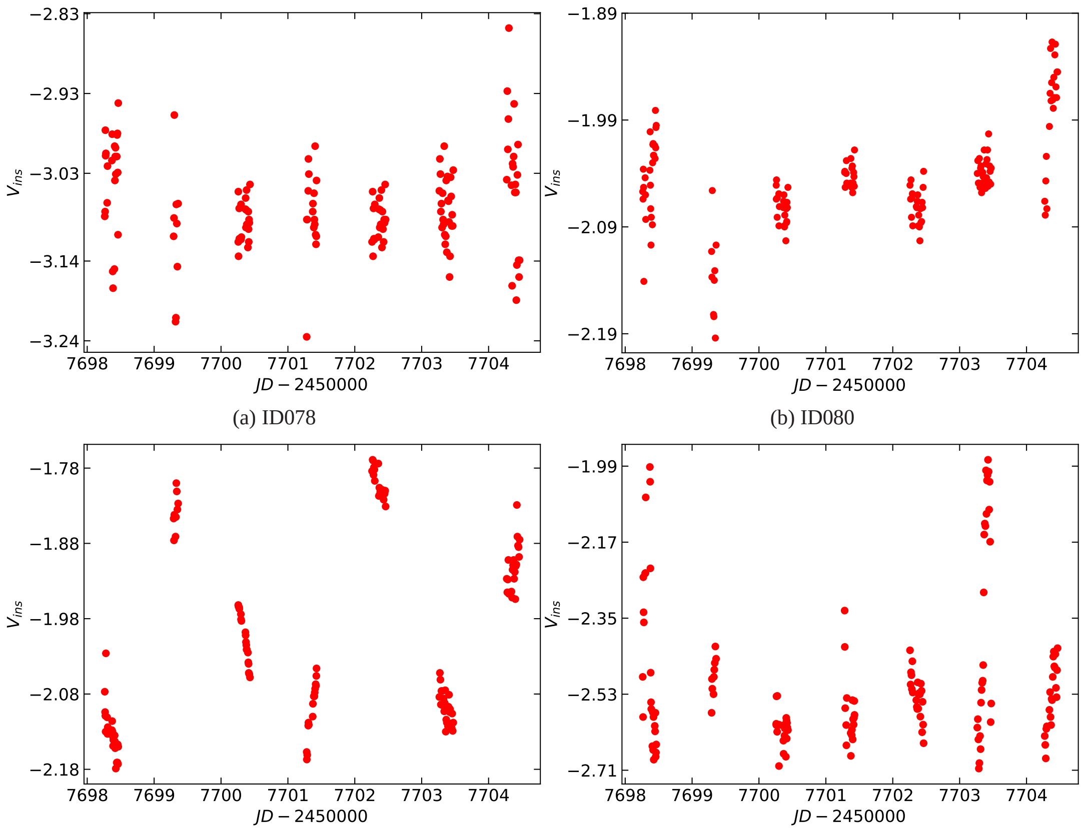

(a) ID078 (b) ID080

(c) ID105 (d) ID126

Fig. 4 Light curves of the four detected variables in the King 1 field.

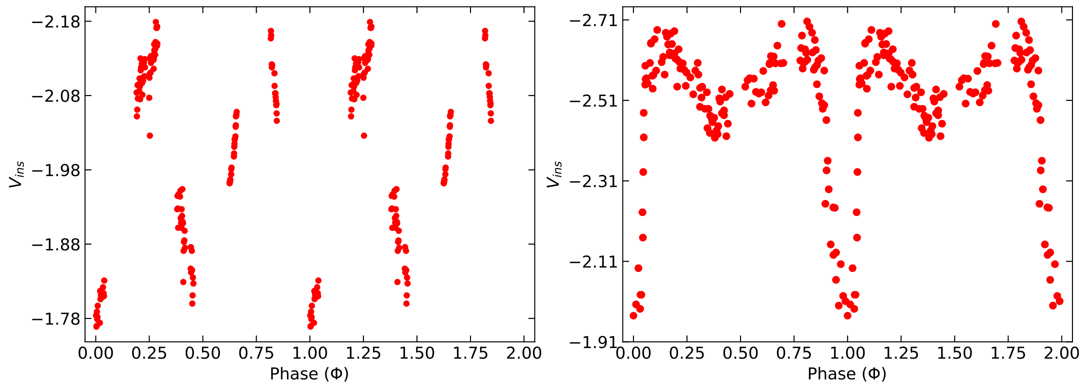

(a) ID105 ($P = 5.31500$ days) (b) ID126 ($P = 0.72538$ days)

Fig. 5 Phased light curves of the binary stars (ID105 and ID126) of the King 1 field. The period value obtained from the PDM and ME methods is utilized to construct the phased plots.

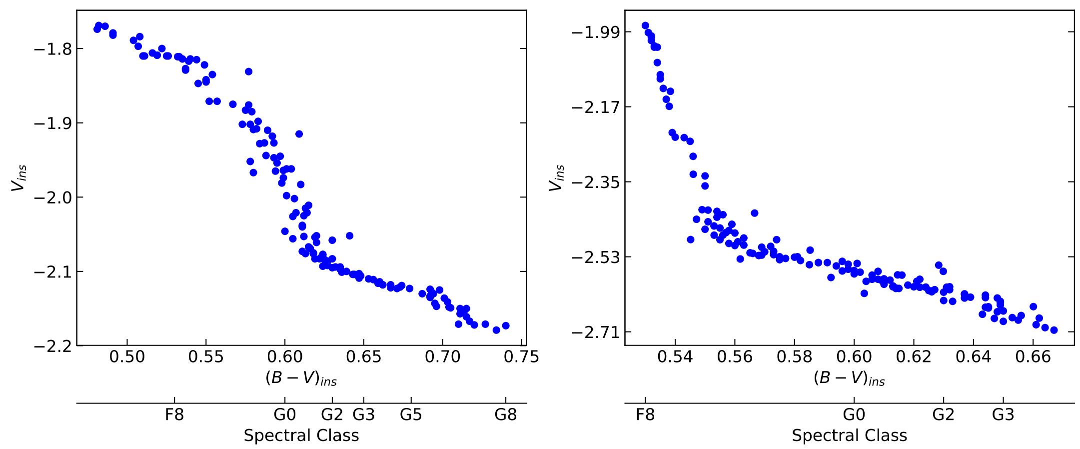

(a) ID105 (b) ID126

Fig. 6 Color-magnitude diagrams of both the binary stars in the open cluster King 1 field. The spectral class axes in both (a) and (b) relate the color $(B-V)$ values to their corresponding spectral class.

(Stellingwerf 1978), and Lomb-Scargle (LS) periodogram (Scargle 1982). PDM and LS are extremely fast and precise methods for determining the most significant period in unevenly sampled data of a variable star (Horne & Baliunas 1986). We have performed periodogram analysis on the four detected variables, covering a frequency range between 0.05 and 100 d^{-1}, with a maximum of 1000 frequency steps in PDM.

The light curves of the four detected variables are depicted in Figure 4. These are visually inspected and phase plots are generated for each of the variable stars, based on the periods obtained from the PDM method.

We are not including the phase plots of ID078 and ID080, since their phase plots point towards aperiodic variations. For ID105 and ID126, the PDM based period gives a less scattered and well arranged phase plot as compared to the periods obtained from LS. The determination of periods is found to improve further by using the entropy minimization (ME) method, as described in Deb & Singh (2011). The ME method is run around $\pm 1\%$ of the periods obtained from PDM. However, both the periods from the PDM and ME methods are ascertained to be nearly identical in the present case. Table 2 contains the detected periods of the four variables, along with their catalog IDs and RA Dec.

5 RESULTS AND CONCLUSIONS

In eclipsing binaries, a portion of light is blocked when one component moves in front of the other one and the flux is diminished. They display particular characteristics and are readily acknowledged by observational data. Vital information, such as radius, mass ratio, inclination angles, temperatures, etc., can be obtained for these types of stars by modeling their variation of light with respect to different phases of eclipses.

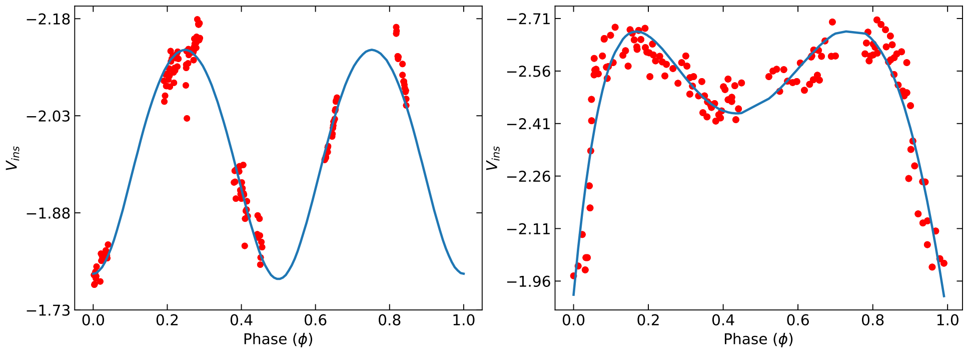

(a) ID105 (b) ID126

Fig. 7 PHOEBE modeling of the binary stars (ID105 and ID126) in the King 1 field.

Table 2 Periods of the variables identified in King 1

Object	RA (hh:mm:ss)	Dec (dd:mm:ss)	Period (PDM)	log(P) (PDM)	Period (LS)	ID (Gaia DR2)	ID (2MASS)
ID078	00:21:55.93	+64:20:58.70	1.1976	0.2957	1.1853	431180635962447104	00215593+6420587
ID080	00:21:54.81	+64:20:58.60	1.5325	0.1854	1.6559	431180635954092288	00215481+6420586
ID105	00:22:03.92	+64:18:37.53	5.3150	0.7255	5.393	431177264404482944	00220394+6418380
ID126	00:21:56.53	+64:25:37.89	0.7253	–0.1390	0.7336	431182422668794880	00215654+6425381

Table 3 Physical parameters of the binary stars in the King 1 field obtained from PHOEBE

Star	i	Ω_1	Ω_2	$q=\frac{m_2}{m_1}$	T_1^e	T_2^e	R_1	R_2	M_2^b	M_1^b	$\log(g)_1$	$\log(g)_2$	SB_1	SB_2	PHSV	PCSV
ID105	51.8	2.987	2.657	0.558	5725	6200	4.676	3.827	1.476	1.565	3.896	3.818	0.048	0.070	4.3	9
ID126	57.5	10.922	10.277	6.445	5578	5700	1.224	4.418	4.499	1.619	4.112	3.807	3.982	0.346	12.5	10

$\Omega_{1,2}$: Luminosity of [1] primary and [2] secondary star; $T^e_{1,2}$: Effective Temperature in K; $\mathrm{SB}_{1,2}$: Surface Brightness; PHSV: Primary Star Surface Potential; PCSV: Secondary Star Surface Potential.

From photometric observation of the King 1 field, we detected four stellar variables, out of which two are found to be binary stars. However, the parallax of these four variables obtained from Gaia DR2 confirms that ID105 and ID126 are not a part of King 1, but rather are located far in front of the cluster, along its line of sight. Figure 5 depicts the phase plot of the detected binaries. To analyze the observed light curves, we utilized PHOEBE based on the Wilson-Devinney (W-D) code (Wilson & Devinney 1971). In PHOEBE, the parameters, such as gravity brightening, limb darkening and bolometric albedo, are kept as default for both the stars. For convective envelopes, the gravity brightening coefficients for binaries are 0.32, whereas the bolometric albedo is taken as 0.6 for both the components. Table 3 lists the photometric solutions obtained for the two detected binaries. The fitted light curves obtained from PHOEBE modeling are displayed in Figure 7. We have followed Lucy (1967) while applying PHOEBE for overcontact binaries.

Mass ratio is a significant parameter for understanding a binary star. W UMa binaries usually have short periods in the range $0.2 < p < 1$ d (Kang et al. 2002; Luo et al. 2017). Based on observational features, W UMa binaries can be divided into two subclasses, i.e., (i) A-type and (ii) W-type. An A-type system with greater luminosity and reduced mass ratio, i.e., $q = M_2/M_1 < 1$ is of spectral type from A to G (Binnendijk 1970). The transit eclipse of the massive hot component manifests deeper minima for a W UMa binary of A-type. The W-type W UMa binary generally exhibits a mass ratio $q = M_2/M_1 > 1$ and a spectral type from F to K. The angle of inclination (i) of the stellar systems ID105 and ID126 are found to be $51.8°$ and $57.5°$ respectively. Stars with inclination $i < 90°$ have counterclockwise rotation, as mentioned in Dar et al. (2018c). The temperature difference ΔT between the components of ID105 and ID126 is 475 K and 122 K respectively. For difference in temperatures between the components $\Delta T \geq 1000$ K, the binary system is classified as B-type W UMa, where the component stars are not in thermal contact, but in geometrical contact with each other (Rucinski & Duerbeck 1997; Deb & Singh 2011). However, from our analysis, we did not find a W UMa binary of B-type, as the temperature difference of both the components is ascertained to be less than 1000 K for ID105 and ID126 respectively.

On the other hand, the period of the binary star ID105 is found to be 5.393 d, which is greater than 1 d, confirming that the binary system cannot be a W UMa. Li et al.

(2007) classified the three types of binary systems, i.e., Eclipsing Contact (EC), Eclipsing Semi-Detached (ESD) and Eclipsing Detached (ED), applying the logarithm of period ($\log$ P) values of the variable stars, where most of the EC, ESD, and ED systems range around ~ -0.455, ~ -0.2 and ~ 0.35 respectively. In our analysis, ID105 and ID126 exhibit $\log$ P values 0.7255 and -0.139 respectively, as mentioned in Table 2. Considering the $\log$ P value and mass ratio of ID105 and ID126, we can conclude that ID105 is an ED, whereas ID126 is an EC binary.

The period, mass ratio and effective temperature of ID126 crowns it to be a newly detected W UMa binary system. Its mass ratio being greater than 1 and spectral type between F to G suggest it to be a W type W UMa binary star. The effective temperatures obtained from PHOEBE modeling range between $5500\,\mathrm{K}$ and $6000\,\mathrm{K}$ for both the binary systems, as mentioned in Table 3. The range of effective temperature is in good agreement with the results obtained from the color-magnitude diagram, as displayed in Figure 6. The color-magnitude diagram in Figure 6 supports the spectral types of both the binary systems, correlating the effective temperatures calculated from the photometric observations with their modeling counterpart obtained from PHOEBE.

We have reported the photometric study of two variables, viz. ID78 and ID80, from the King 1 cluster and two binary systems, viz. ID105 and ID126 in the King 1 field, along the line of sight of the open cluster. Though the results reported are definitely going to add value to the understanding of this relatively less studied cluster, coupling spectroscopic as well as polarimetric results with it would enhance our insight into the field.

Acknowledgements PRS and DH are thankful to MHRD TEQIP-III for awarding fellowships for pursuing Ph.D.s at Gauhati University. PRS and AAD are also grateful to the Director, Indian Institute of Astrophysics (IIA), Bangalore for providing observation time at Vainu Bappu Observatory. A hearty thanks go to the anonymous referee for carefully examining the manuscript, helping us to explore new dimensions in the study and adding value to the work.

This work has made use of data from the European Space Agency (ESA) mission *Gaia* (`https://www.cosmos.esa.int/gaia`), processed by the *Gaia* Data Processing and Analysis Consortium (DPAC, `https://www.cosmos.esa.int/web/gaia/dpac/consortium`). Funding for the DPAC has been provided by national institutions, in particular the institutions participating in the *Gaia* Multilateral Agreement.

References

Binnendijk, L. 1970, Vistas in Astronomy, 12, 217
Carrera, R., Rodríguez Espinosa, L., Casamiquela, L., et al. 2017, MNRAS, 470, 4285
Dar, A. A., Parihar, P. S., Saleh, P., & Malik, M. A. 2018a, New Astron., 64, 34
Dar, A. A., Singh Parihar, P., & Malik, M. A. 2018b, RAA (Research in Astronomy and Astrophysics), 18, 112
Dar, A. A., Singh Parihar, P., Saleh, P., & Malik, M. A. 2018c, RAA (Research in Astronomy and Astrophysics), 18, 155
Deb, S., & Singh, H. P. 2011, MNRAS, 412, 1787
Gaia Collaboration, Brown, A. G. A., Vallenari, A., et al. 2018, A&A, 616, A1
Gilliland, R. L., & Brown, T. M. 1988, PASP, 100, 754
Hasegawa, T., Sakamoto, T., & Malasan, H. L. 2008, PASJ, 60, 1267
Horne, J. H., & Baliunas, S. L. 1986, ApJ, 302, 757
Kang, Y. B., Kim, S. L., Rey, S. C., et al. 2007, PASP, 119, 239
Kang, Y. W., Oh, K.-D., Kim, C.-H., et al. 2002, MNRAS, 331, 707
King, I. 1949, Harvard College Observatory Bulletin, 919, 41
Kiss, L. L., Szabó, G. M., Sziládi, K., et al. 2001, A&A, 376, 561
Lata, S., Mohan, V., & Sagar, R. 2004, Bulletin of the Astronomical Society of India, 32, 371
Lata, S., Pandey, A. K., Maheswar, G., Mondal, S., & Kumar, B. 2011, MNRAS, 418, 1346
Lata, S., Yadav, R. K., Pandey, A. K., et al. 2014, MNRAS, 442, 273
Li, L., Zhang, F., Han, Z., & Jiang, D. 2007, ApJ, 662, 596
Lucy, L. B. 1967, ZAp, 65, 89
Luo, C., Zhang, X., Deng, L., et al. 2017, New Astron., 52, 29
Maciejewski, G., & Niedzielski, A. 2007, A&A, 467, 1065
Rucinski, S. M., & Duerbeck, H. W. 1997, in ESA Special Publication, 402, Hipparcos - Venice '97, eds. R. M. Bonnet, E. Høg, P. L. Bernacca, et al. 457
Scargle, J. D. 1982, ApJ, 263, 835
Stellingwerf, R. F. 1978, ApJ, 224, 953
Stetson, P. B. 1987, PASP, 99, 191
Wang, K., Deng, L., Zhang, X., et al. 2015, AJ, 150, 161
Wilson, R. E., & Devinney, E. J. 1971, ApJ, 166, 605